Available online at www.sciencedirect.com
SCIENCE DIRECT®
Biochemical Pharmacology 67 (2004) 2187–2196
Biochemical Pharmacology
www.elsevier.com/locate/biochempharm

The cystic fibrosis mutation G1349D within the signature motif LSHGH of NBD2 abolishes the activation of CFTR chloride channels by genistein

Patricia Melin, Vincent Thoreau, Caroline Norez, Frédéric Bilan, Alain Kitzis, Frédéric Becq*

Institut de Physiologie et Biologie Cellulaires CNRS UMR 6187, Université de Poitiers, 40 Avenue du Recteur Pineau, 86022 Poitiers, France

Received 27 October 2003; accepted 5 February 2004

Abstract

Cystic fibrosis (CF) is a common lethal genetic disease caused by autosomal recessive mutations of the cystic fibrosis transmembrane conductance regulator (CFTR) chloride channel that belongs to the ATP-Binding Cassette (ABC) family of transporters. The class III CF mutations G551D and G1349D are located within the ''signature'' sequence LSGGQ and LSHGH of NBD1 and NBD2, respectively. We have constructed by site-directed mutagenesis vectors encoding green fluorescent protein (GFP)-tagged wild-type (wt) CFTR or CFTR containing delF508, G551D, G1349D and G551D/G1349D to study their pharmacology after transient expression in COS-7 cells. We show that IBMX and the benzo[c]quinolizinium derivative MPB-91 stimulates the activity of G1349D-, G551D- and G551D/G1349D-CFTR only in the presence of cAMP-promoting agents like forskolin or cpt-cAMP. Similar half-maximal effective concentrations (EC_{50}) of MPB-91 (22–36 μM) have been determined for wt-, G551D-, G1349D- and G551D/G1349D-CFTR. The isoflavone genistein stimulates wild-type (wt)- and delF508-CFTR channel activity in a non-Michaelis–Menten manner. By contrast, the response of G1349D- and G551D-CFTR to genistein is dramatically altered. First, genistein is not able to stimulate G1349D- and G551D/G1349D-CFTR. Second, genistein stimulates G551D-CFTR without any inhibition at high concentration. We conclude from these results that whereas G551 in NBD1 is an important molecular site for inhibition of CFTR by genistein, the symmetrical G1349 in NBD2 is also one major site but for the activation of CFTR by genistein. Because both mutations alter specifically the mechanism of CFTR channel activation by genistein, we believe that the signature sequences of CFTR act as molecular switches that upon interaction with genistein turn on and off the channel.

Keywords: CFTR; Signature sequences; Genistein; G1349D; G551D; delF508

1. Introduction

ATP-binding cassette (ABC) transporters are members of a large family of membrane proteins that catalyse the active transport of a variety of solutes across biological membranes [1]. ABC tranporters are composed of two repeated units joined by a linker region [1]. Each part has six transmembrane segments and a hydrophilic domain containing an ATP-binding site, the nucleotide binding domain (NBD). NBD contains highly conserved Walker A and B motifs in common to a variety of ATP-binding proteins [2]. The LSGGQ motif (also named ''linker peptide'' or ''signature sequence'') shows remarkable conservation in NBDs of all ABC transporters and is interposed between the two Walker domains [1]. The function of this sequence is still largely unknown. Recent studies revealed however that the conserved sequence in each NBD interacts with the Walker A consensus nucleotide-binding domain in the opposite NBD [3–9].

The cystic fibrosis transmembrane conductance regulator (CFTR), the protein product of the *CFTR* gene, is an ABC transporter (ABCC7) with unique properties of cAMP-regulated chloride channel [10]. Cystic fibrosis

Abbreviations: ABC, ATP-binding cassette; CF, cystic fibrosis; CFTR, cystic fibrosis transmembrane conductance regulator; GFP, green fluorescent protein; Gst, genistein; Fsk, forskolin; NBD1 and NBD2, nucleotide binding domain 1 and 2; DIDS, 4,4′-diisothiocyanatostilbene-2,2′-disulfonic acid; MPB-91, 5-butyl-6-hydroxy-10-chlorobenzo[c]quinolizinium chloride

* Corresponding author. Tel.: +33-5-49-45-37-29; fax: +33-5-49-45-40-14.
E-mail address: frederic.becq@univ-poitiers.fr (F. Becq).

0006-2952/$ – see front matter © 2004 Elsevier Inc. All rights reserved.
doi:10.1016/j.bcp.2004.02.022

(CF), one of the most common lethal autosomal recessive genetic disease, is caused by mutations of the *CFTR* gene at the origin of defective Cl^- transport across the affected epithelium [11,12]. CFTR mutations (http://www.genet.sickkids.on.ca/cftr) can be assigned to one of five classes of mutations [13], leading to a protein which chloride channel function is altered (classes III and IV) or lacking (classes I, II and V) at the apical membrane. The glycine-to-aspartic acid missense mutations G551D and G1349D are class III mutations located within the signature sequence LSGGQ in NBD1 and LSHGH in NBD2, respectively [13–15]. G551D is one of the five most frequent CF mutation with a frequency of 2–5% depending of the population of origin. Class III mutations disrupt activation and regulation of CFTR at the plasma membrane and lead to a severe CF phenotype [13,14,16]. However, class III CFTR channels are fully glycosylated, correctly located at the apical plasma membrane and normally phosphorylated at the R domain by cAMP-dependent protein kinases [14–18]. The most common CF mutation (delF508, class II), leading to a severe CF phenotype, is a three base pair deletion resulting in loss of a phenylalanine residue at position 508 in the protein [10,11,13,14]. Trafficking of delF508 mutants from the endoplasmic reticulum (ER) to the apical plasma membrane of epithelial cells is extremely inefficient. Therefore, cells expressing delF508-CFTR show severely reduced Cl^- channel activity compared to wt, since the protein is incorrectly processed (no glycosylation) and retained within the ER [10,11,13].

We have demonstrated recently that the glycine G551 in the LSGGQ motif of CFTR is the key amino acid for inhibition of CFTR chloride channel activity by high concentration of genistein [19]. In this study, we used site-directed mutagenesis and pharmacological analysis of CFTR channel activity to search for the activatory genistein binding site. Our results show that mutation of the symmetrical glycine G1349 into aspartate in the LSHGH motif of the second NBD abolished CFTR activation by genistein demonstrating that G1349 is part of the activatory genistein binding site. The opposite role of both symmetrical glycines of the signature sequences is discussed at the light of the recent model proposed for the NBD dimerization of ABC transporters [3–9,20].

2. Materials and methods

2.1. Site-directed mutagenesis of CFTR

GFP-tagged CFTR expression was used. Mutations were introduced into pS65T/EGFP-C1/wt-CFTR construct [21] provided generously by K.H. Karlson (Dartmouth College, Hanover, NH) by oligonucleotide-directed mutagenesis using QuickChange® XL Site-Directed Mutagenesis Kit (Stratagene). The delF508, G551D and G1349D mutations were created using the sense oligonucleotides 5′-CATTAAAGAAAATATCATTGGTGTTTCCTATGATG-3′, 5′-GGAATCACACTGAGTGGAGATCAACGAGCAAGAATTTCTT-3′ and 5′-GGCTGTGTCCTAAGCCATGACCACAAGCAGTTGATGTGC-3′, respectively, and the corresponding antisense oligonucletotides. Double mutant G551D/G1349D was derived from G551D. Mutations in individual clones were verified through plasmid sequencing on both strands using the ABI PRISM Big Dye Terminator™ Cycle Sequencing Ready Reaction Kit (Applied Biosystems). Reactions were run on an ABI PRISM™ 310 automatic sequencer (Applied Biosystems).

2.2. Transient transfection of mutant CFTR

Subconfluent COS-7 cells (50,000 cells per well) were transfected with the cDNA constructs with 0.5 μg of plasmid using cationic lipids (JetPEI, Qbiogene). The media was replaced 24 h post-transfection. COS-7 cells were either transfected with empty pEGFP-C1 vector (mock) or with expression vector encoding wild-type GFP-tagged CFTR (wt-CFTR), or mutant forms of GFP-CFTR: delF508, G551D, G1349 or the double mutant G551D/G1349D (named 2GD-CFTR). Fluorescence was detected using confocal laser scanning microscopy on a Biorad MRC 1024.

2.3. Western blot analysis

COS-7 cell lysates (50 mM Tris–HCl, pH 7.5, 1 mM EDTA, 100 mM NaCl, 1% Triton X-100, 20 μM leupeptin, 10 μM pepstatin, 0.8 μM aprotinin, 2.1 mM AEBSF) were separated 48 h after transfection by 7% polyacrylamide SDS-PAGE (30 μg protein per lane) and transferred to nitrocellulose membrane (Sartorius). Membrane was incubated overnight at 4 °C in Phosphate-Buffered Saline, 0.1% Tween 20, with 2 μg/ml of mouse anti-CFTR monoclonal antibody (clone M3A7, Chemicon International). Horseradish peroxydase-conjugated sheep anti-mouse IgG (1:3000; Amersham Pharmacia Biotech) was used as secondary antibody and revealed with ECL Western Blotting Detection Reagent (Amersham Pharmacia Biotech).

2.4. Examination of distribution of GFP-CFTR by confocal microscopy

COS-7 cells were washed 72 h after transfection, in TBS (NaCl 157 mM, Tris 20 mM, 300 mOsmol, pH 7.4) and fixed in paraformaldehyde (3% in TBS). Nuclei were stained with TOPRO-3 iodide (1:1000 in TBS, Molecular Probes). Coverglasses containing cells were mounted in appropriate medium (Vectashield®, Vector Laboratories). Images were acquired using a reversed microscope (Olympus IX 70) equipped with a laser scanning confocal unit (model MRC-1024, BioRad), a 15 mW krypton-argon laser, and a ×60 water immersion objective. GFP fluorescence was excited using the 488 nm laser line and

collected using a standard fluorescein isothiocyanate filter set (522 ± 32 nm). Fluorescence associated with TOPRO-3 iodide was excited using the 647 nm laser line and collected using a filter set (680 ± 32 nm). Double fluorescence images were generated simultaneously.

2.5. Iodide efflux experiments

CFTR chloride channel activity was assayed by measuring the rate of iodide (^{125}I) efflux versus time from COS-7 cells at 72 h post-transfection. All experiments were performed at 37 °C and analysed as previously described [19]. Iodide efflux curves were constructed by plotting rate (k, min^{-1}) of ^{125}I versus time. Concentration-dependent activation curves were constructed by plotting the maximal value for the time-dependent rate (peak rates) excluding the third point used to establish the baseline (noted k peak-k basal, min^{-1}) [19]. The benzo[c]quinolizinium compound MPB-91 (5-butyl-6-hydroxy-10-chlorobenzo[c]quinolizinium chloride) was prepared as described previously [22] by Dr Y. Mettey (Laboratoire de chimie organique, Poitiers, France). DIDS (4,4′-diisothiocyanatostilbene-2,2′-disulfonic acid) was from Sigma Chemicals. All other products were from Sigma. All compounds were dissolved in dimethylsulfoxide (DMSO, final concentration: 0.1%).

2.6. Statistics

Results are expressed as mean ± S.E.M. of n observations. Sets of data were compared with either an analysis of variance (ANOVA) or Student's t test. Differences were considered statistically significant when $P < 0.05$. Non significant (ns) difference, $^{*}P < 0.05$, $^{**}P < 0.01$, $^{***}P < 0.001$. All statistical tests were performed using GraphPad Prism version 3.0 for Windows (GraphPad Software).

3. Results

To study the pharmacology of CFTR, we have introduced green fluorescent protein (GFP)-tagged CFTR proteins into COS-7 cells, i.e. wt-CFTR and four CFTR mutants i.e. delF508, G551D, G1349D and the double mutant G551D/G1349D (named 2GD). The glycines, conserved throughout ABC transporters [3], lie within the signature sequence LSGGQ in NBD1 and LSHGH in NBD2 (Fig. 1A). GFP-CFTR proteins were detected by western blot analysis using CFTR NBD2 C-terminal antibodies (Fig. 1B). Control experiments were performed using either non-transfected or mock-transfected COS-7 cells (Fig. 1B, lanes 1 and 2, respectively). GFP-wt-CFTR from cell lysates migrated as two bands at 210 and 240 kDa (lane 3) corresponding to the core-glycosylated band B and mature-glycosylated band C, respectively [21]. Western blot analysis of GFP-delF508 mutant shows the absence of the band C (lane 4), as expected for a protein having an altered trafficking [10,13]. GFP-G1349D (lane 5), GFP-G551D/G1349D (lane 6) and GFP-G551D (lane 7) appeared with a similar pattern like the non-mutated form of CFTR (lane 3). Confocal fluorescence microscopy confirmed the membrane location of the different constructions (Fig. 1C) except for GFP-delF508 that was found restricted to intracellular compartments with cells cultured at 37 °C.

The chloride channel activity of these proteins have been studied by radiotracer flux analysis after transient expression in COS-7 cells. We began our functional comparison by examining several basic pharmacological properties. As shown Fig. 2A, only the transport activity of GFP-wt-CFTR channels was stimulated by 10 μM forskolin ($n = 4$) as previously reported for wt-CFTR without GFP tag [19,21]. The two mutated channels G1349D- and 2GD-CFTR, like G551D-CFTR, did not respond to forskolin stimulation ($n = 4$ for each construct, Fig. 2A), as expected from class III CF mutations [13,19]. However, when a cAMP cocktail composed of forskolin, IBMX and cpt-cAMP was used instead of forskolin alone, the chloride channel activity of G1349D and 2GD mutants was stimulated, indicating that both proteins have functional cAMP-dependent chloride channel activity ($n = 4$, Fig. 2B and C) like G551D-CFTR (data not shown and [19]). The pharmacological profile for inhibition of these mutants was then compared using different chloride channel inhibitors, i.e. the sulfonylurea drug glibenclamide and the stilbene disulfonate derivative DIDS. These agents have been chosen because previous studies demonstrated that glibenclamide but not DIDS inhibits CFTR channel activity [reviewed in [10]]. We were able to confirm this typical signature using 100 μM glibenclamide and 500 μM DIDS. Only glibenclamide inhibited the chloride channel activity of G1349D- and 2GD-CFTR (Fig. 2B and C). Note that the vehicle DMSO has no apparent effect on the iodide efflux (Fig. 2D) A summary of the data obtained with glibenclamide and DIDS is presented Fig. 2E for wt-, G1349D- and 2GD-CFTR stimulated by cAMP cocktail.

In a second set of experiments, we used the benzoquinolizinium drug MPB-91, a CFTR pharmacological agent already shown to activate wt and G551D-CFTR [22]. Fig. 3 presents concentration-dependent activation for the different constructs. We found that MPB-91 stimulated the iodide efflux with similar EC_{50} of 29 ± 1.4, 22 ± 1.4, 22 ± 1.3 and 36 ± 1.1 μM for wt-, G551D-, G1349D and 2GD-CFTR, respectively ($n = 4$ for each concentration). We also found that G1349D and the double mutant 2GD could be stimulated by forskolin and 100 μM IBMX (not shown) as previously reported by others [23,24].

The response to genistein of wt-CFTR was then compared to that of the mutated proteins at glycine residue. In the presence of genistein, the pharmacological behaviour of wt-CFTR is characterized by a non-Michaelis–Menten behaviour [19]. We first verified this property with GFP-

Walker A signature Walker B

NBD1 …[458]GSTGAGKT[465]… [548]LSGGQ[552]… [561]AVYKD[565]…

NBD2 …[1244]GRTGSGKS[1251]…[1346]LSHGH[1350]…[1364]ILLLD[1370]…

(A)

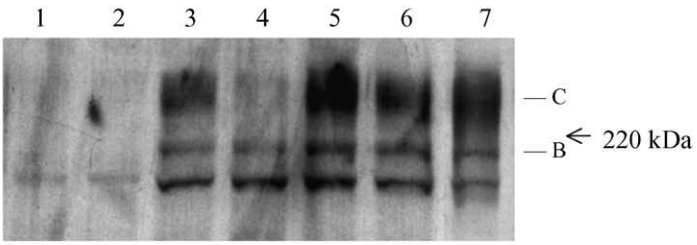

(B)

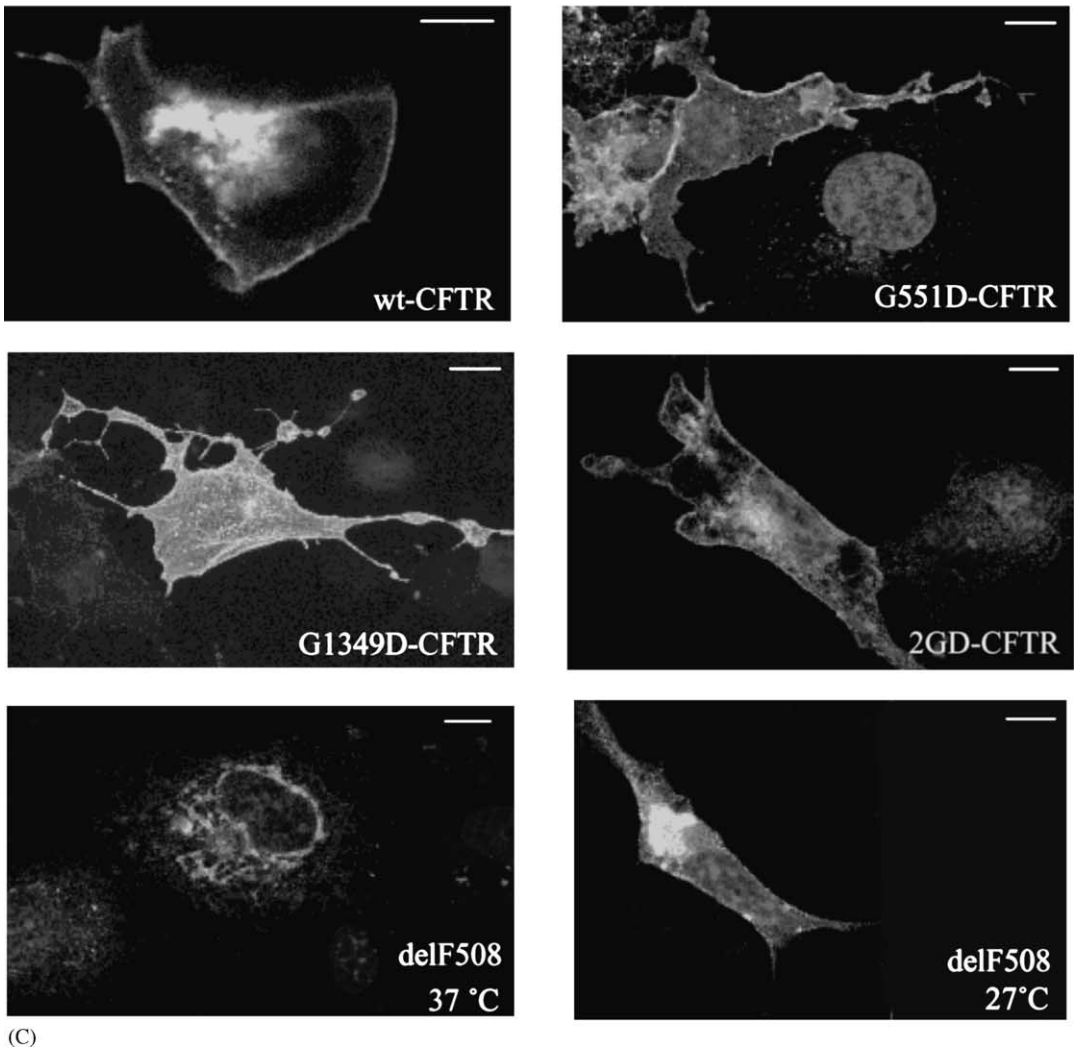

(C)

Fig. 1. Expression of wt- and mutant CFTR channels. (A) alignment of Walker A, Walker B and signature sequences for NBD1 and NBD2 of the human CFTR protein with the amino-acid positions. The glycine G551 and G1349 are underlined in bold. (B) western blot analysis of the GFP-CFTR expression detected with CFTR NBD2 C-terminal antibody. On the right is indicated the position of bands B and C; band B, 210-kDa core-glycosylated GFP-CFTR and band C, 240-kDa mature-glycosylated GFP-CFTR. Lane 1: non transfected COS-7 cells; lane 2: mock-transfected cells; lane 3: GFP-wt-CFTR, lane 4: GFP-delF508-CFTR; lane 5: GFP-G1349D-CFTR; lane 6: GFP-2GD-CFTR; lane 7: GFP-G551D-CFTR. (C) confocal imaging showing plasma membrane localization of wt-CFTR, G551D-, G1349D- and 2GD-CFTR. The delF508 mutant at 37 °C (bottom left) is restricted to intracellular compartments whereas at 27 °C (bottom, right) it becomes localized at the plasma membrane. Scale bar is 10 μm.

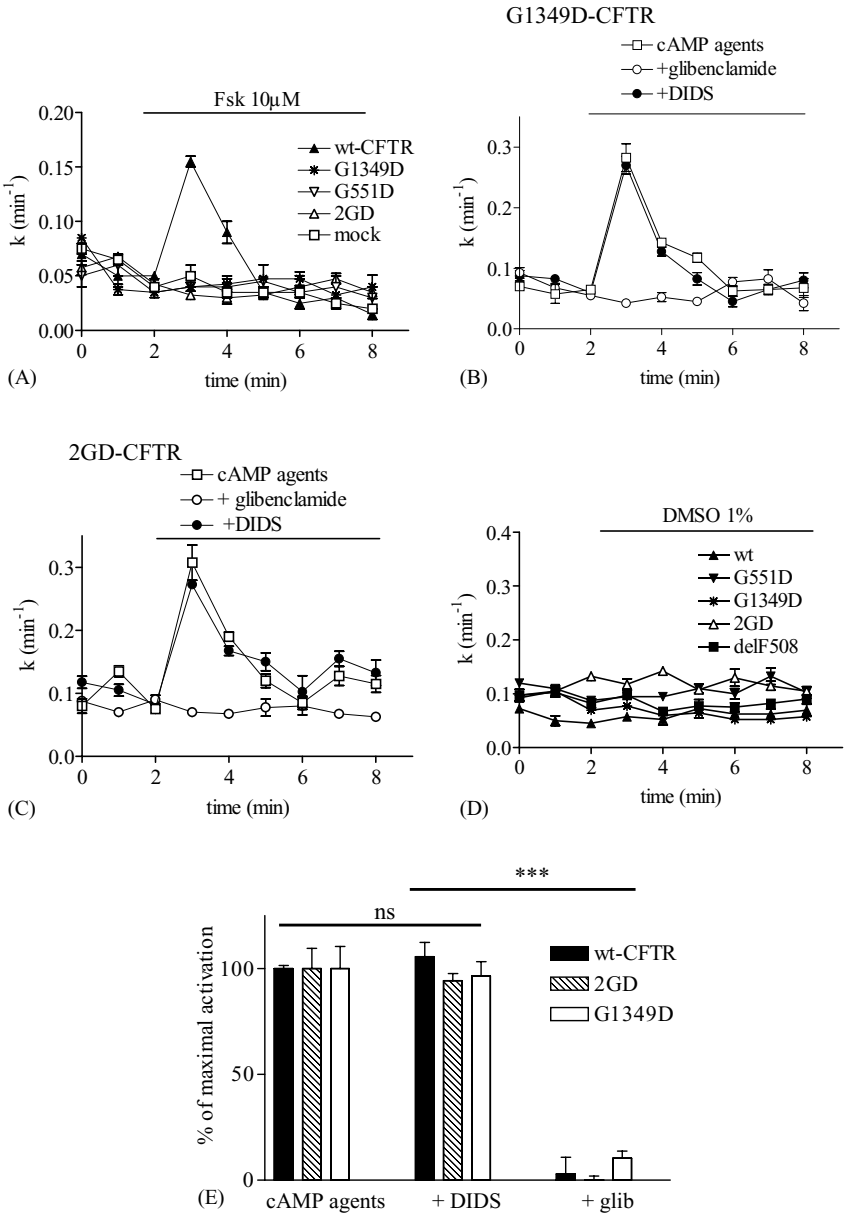

Fig. 2. Functional expression and pharmacology of GFP-tagged wt-, G551D-, G1349D- and 2GD-CFTR. (A) time-dependent iodide efflux curves showing the stimulation of CFTR channels by 10 µM forskolin (noted Fsk). B and C, analysis of the expression of G1349D-CFTR (B) and 2GD-CFTR (C) mutants in COS-7 cells. The cAMP agents are 10 µM forskolin, 500 µM IBMX and 500 µM cpt-cAMP. Note that 100 µM glibenclamide but not 500 µM DIDS inhibited the cAMP-dependent activation of iodide efflux for both proteins. (D) effect of the vehicle DMSO used at 1% in this study as indicated for the different constructs. (E) summary of the % of maximal activation in the presence of glibenclamide and DIDS for wt-, G1349D and 2GD-CFTR, as indicated. Data are presented as mean ± S.E.M. $n = 4$ for each experimental condition. $^{***}P < 0.001$; ns: non significant difference. Some error bars are smaller than the symbol. Horizontal bar above traces in A–D indicates the presence of agonists, inhibitors or vehicle.

wt-CFTR. Cells were stimulated by 500 nM forskolin and by increasing concentrations of genistein from 3 to 300 µM ($n = 4$ for each concentration, Fig. 4A). For concentrations up to 30 µM, genistein stimulated GFP-wt-CFTR (Fig. 4A, left traces) but for higher concentrations, i.e. 300 µM genistein, an inhibition of the channel activity was evidenced (Fig. 4A, right traces). Note that even at 100 µM genistein the stimulation of wt-CFTR was attenuated (although not statistically different from that obtained with 30 µM). The corresponding bell-shaped relationship is presented Fig. 4E and shows the existence of the two opposite effects of genistein as described elsewhere [19]. Fig. 4B shows that the G551D mutation altered the non-Michaelis–Menten behaviour of GFP-wt-CFTR in such a way that the inhibitory effect of genistein at high concentration was abolished (Fig. 4B, right traces). The corresponding concentration-dependent activation relationship is presented Fig. 4E (superimposed to that of wt-CFTR for comparison). The calculated half-maximal effective concentration EC_{50} was 13 ± 1.25 µM ($n = 4$), in perfect agreement with the value of 11 µM determined in our previous study using CHO cells stably expressing

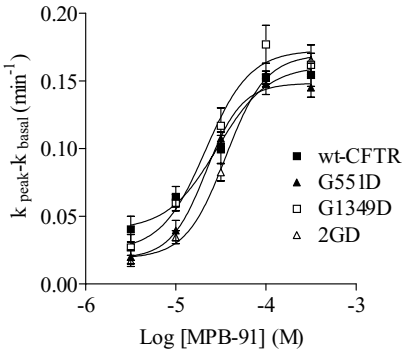

Fig. 3. Effect of the benzoquinolizinium activator MPB-91 on GFP-tagged wt-, G551D-, G1349D- and 2GD-CFTR chloride channel activity. Concentration–response curve for each GFP-tagged CFTR protein stimulated by increasing concentrations of MPB-91 and a fixed concentration of forskolin. Note that for wt-CFTR, 500 nM forskolin was used whereas 10 μM forskolin was required for the three mutants. For each concentration the relative rate was calculated as $k_{peak} - k_{basal}$. Calculated EC_{50} are 29 ± 1.4 μM (wt-CFTR), 22 ± 1.4 μM (G551D-), 22 ± 1.3 μM (G1349D-), and 36 ± 1.1 μM (2GD-CFTR). $n = 4$ for each concentration. Some error bars are smaller than the symbol.

G551D-CFTR [19]. On the contrary, analysing the effect of genistein on the channel activity of the LSHGH mutant G1349D and of the double mutant 2GD demonstrated their inability to be stimulated even in the presence of 10 μM forskolin and 300 μM genistein. Evidence for that is provided Fig. 4C–E. Lack of response given by G1349D-expressing cells was observed in the presence of six different concentrations of genistein (with 10 μM forskolin) and was not statistically different from the control, i.e. with forskolin but without genistein. Similarly, with the double mutant 2GD, 30 μM genistein and 10 μM forskolin added together did not stimulate iodide efflux (Fig. 4D). The corresponding concentration-dependent activation relationships for wt, G551D and G1349D are superimposed on the same graph in Fig. 4E. When compared to the response given by wt-CFTR, the mutation of G1349 abolished the activatory phase while mutation of G551 abolished the inhibitory phase. Since there is no shift to the right of the curve for G1349D, we concluded that the mutant CFTR was fully refractory to genistein stimulation.

Finally, similar experiments were conducted with CFTR chloride channels having the class II CF mutation delF508 because this mutation belongs to a different class of mutation but causes, like G551D and G1349D, a severe CF phenotype. The expression of the mutant protein in COS-7 was verified by western blot analysis (Fig. 1B, lane 4). The delF508 channel activity was studied after 24 h incubation of cells at 27 °C; a protocol known to alter the intracellular processing of delF508, re-directing the mutant protein towards the plasma membrane [25]. The membrane location of delF508 proteins was then verified by confocal imaging (Fig. 1C). With cells cultured at 27 °C, the addition to the bath of genistein, in the presence of 500 nM forskolin, restored delF508 channel activity as shown in Fig. 5A. Interestingly, with increasing concentrations of genistein, delF508-CFTR behaves like wt-CFTR, i.e. with a non-Michaelis–Menten behaviour. Inspection of concentration-dependent relationships presented in Fig. 5B indicates however that the magnitude of the response of delF508-CFTR to genistein was reduced compared to that of wt-CFTR.

In conclusion, we have studied the pharmacology of CFTR chloride channel and the consequence of the three severe CF mutations, delF508, G551D and G1349D. We found a dramatic modification of the pharmacological behaviour of CFTR only with the class III mutations G551D and G1349D that appears to be restricted to genistein. The mechanism of activation (and inhibition) by genistein is apparently not altered by the NBD1 CF mutation delF508.

4. Discussion

This study shows for the first time how two symmetrical CF mutations modify the pharmacological properties of CFTR. We found that glycine G1349 located in the signature sequence LSHGH of NBD2 is a key molecular site for genistein leading to stimulation of the CFTR chloride channel activity. The glycine-to-aspartic acid missense mutation at codon 1349 (class III) causes a severe cystic fibrosis [13,14] and abolishes the pharmacological activation of the chloride channel activity of CFTR by the isoflavone genistein but not by the xanthine IBMX nor by the benzo[c]quinolizinium MPB-91. Recent studies from our group described an unexpected and singular property of CFTR, the non-Michaelis–Menten behaviour, pointing out to the existence of one activatory site and one inhibitory site for genistein [19]. Our previous study on G551D, the symmetrical glycine mutation located in the LSGGQ signature sequence of NBD1, showed that the mutation abolished only the inhibitory genistein effect [19]. Therefore, the results presented here further emphasise the crucial role played by the two signature sequences of CFTR in the regulation of its channel activity.

The class II CF mutation delF508 produced a protein that is functional after its insertion into the plasma membrane [10]. Using the low-temperature protocol we were able to correct the abnormal trafficking defect in delF508-expressing COS-7 cells. Indeed, we found that delF508, like wt-CFTR, behaves in a similar way with respect to the stimulation by genistein, i.e. with a non-Michaelis–Menten behaviour. The magnitude of the response with delF508 was reduced, however, compared to that of wt-CFTR, an observation in agreement with previous reports demonstrating alteration of kinetic parameters of the mutant channel [26]. However, we found that the maximal stimulation of delF508 was obtained at the same concentration of genistein than with wt-CFTR, i.e. 30 μM. Thus, deleting the phenylalanine at position 508, which alters the gating mechanism of the channel and the intracellular trafficking process of the protein, has no apparent effect

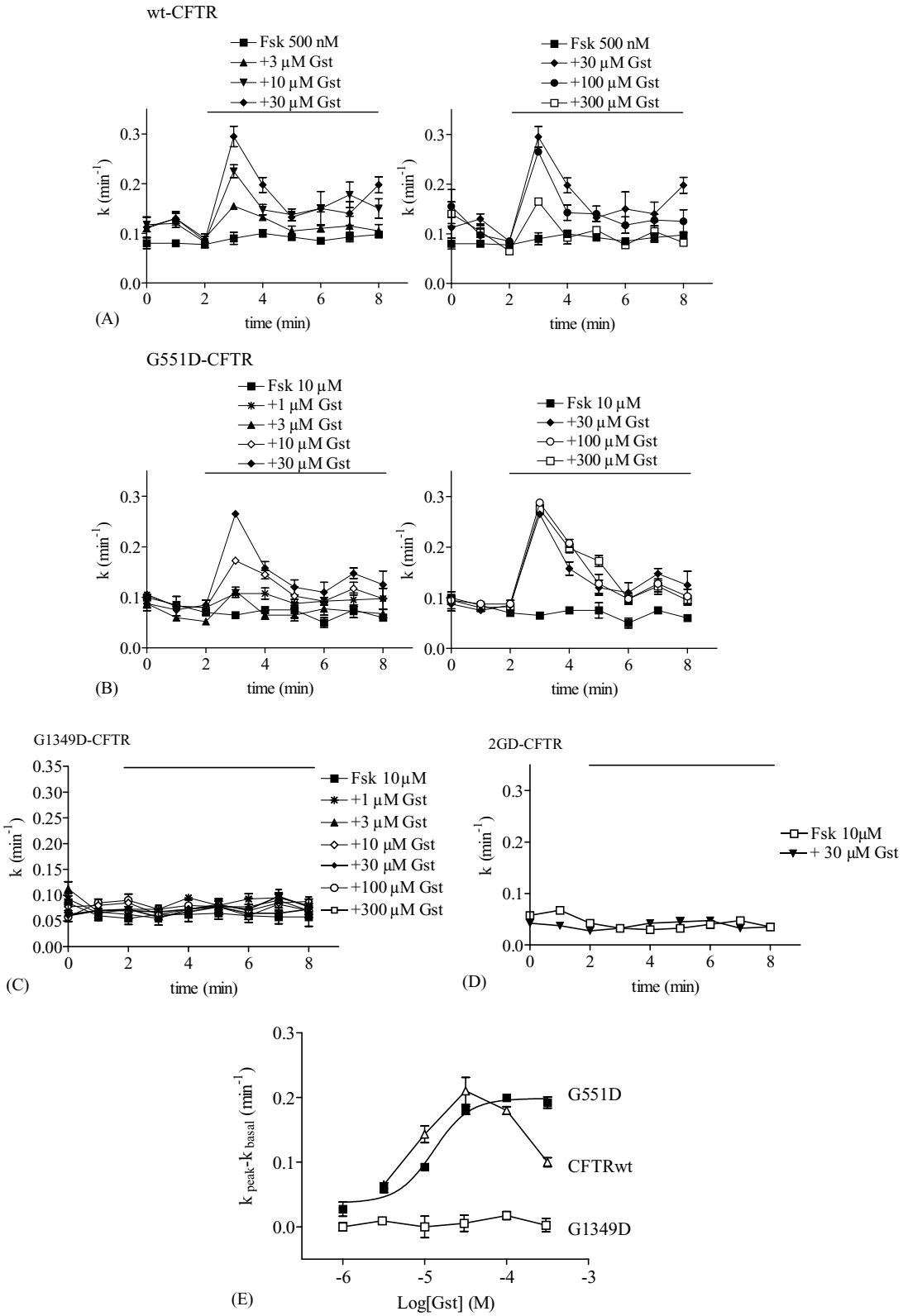

Fig. 4. Effect of genistein on GFP-tagged wt-, G551D-, G1349D- and 2GD-CFTR chloride channel activity. Iodide efflux curves calculated in response to forskolin and various concentrations of genistein with COS-7 cells transiently expressing GFP-CFTR channels: wt- (A), G551D- (B), G1349D- (C) and 2GD- (D). Note that for wt-CFTR 500 nM forskolin was used whereas for the mutants 10 μM forskolin was required. The bar above traces indicates the presence of agonist and its concentration. Data are presented as mean ± S.E.M., $n = 4$ for each experimental condition. (E) Concentration-response curve for each GFP-tagged CFTR construct as indicated. For each concentration the relative rate was calculated as $k_{peak} - k_{basal}$. Note that only for wt-CFTR a bell-shaped relationship was obtained. Some error bars are smaller than the symbol.

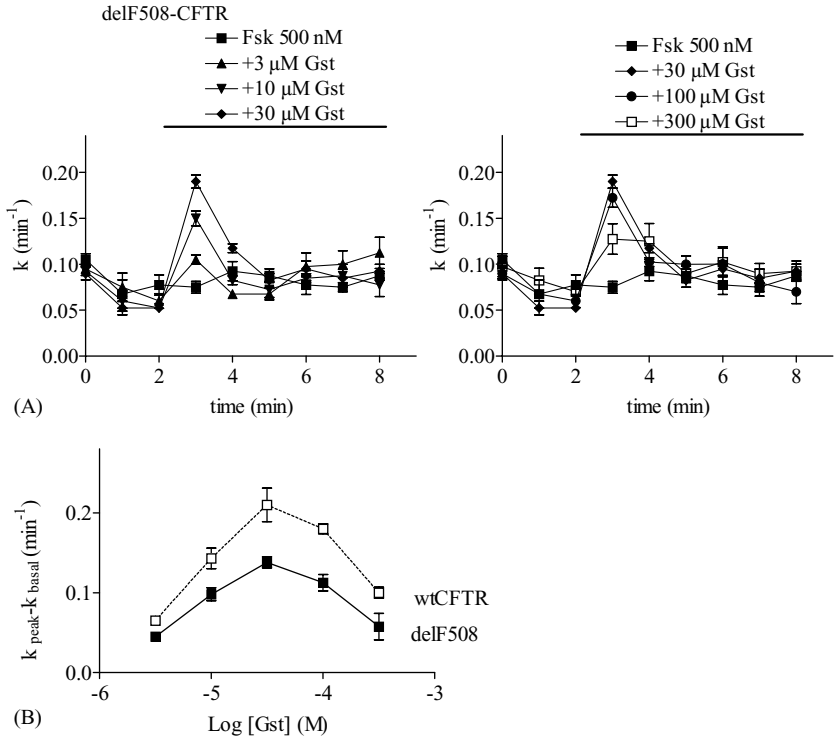

Fig. 5. Non-Michaelis–Menten behaviour of delF508-CFTR chloride channel activity in response to genistein. (A) Iodide efflux curves calculated in response to 500 nM forskolin with various concentrations of genistein for COS-7 cells transiently expressing GFP-delF508-CFTR channels. The bar above traces indicates the presence of agonist and its concentration. Data are presented as mean ± S.E.M., $n = 4$ for each experimental condition. (B) Corresponding concentration-response curves as indicated. For each concentration, the relative rate was calculated as $k_{peak} - k_{basal}$. Note that the response of delF508-CFTR to genistein, like for wt-CFTR, is bell-shaped. We have indicated by a dotted curve the response for wt-CFTR to facilitate the comparison (data taken from Fig. 4E). Note that the magnitude of the response for the mutant is reduced compared to that of the non-mutated protein. Some error bars are smaller than the symbol.

on the mechanism of activation at low concentration nor on the mechanism of inhibition at high concentration of genistein.

Interestingly, within CFTR, the two LSGGQ motifs are different. In NBD1, the signature sequence LSGGQ is strictly conserved, while in NBD2 the symmetrical sequence LSHGH is degenerated. Indeed, CFTR is unique among the ABC transporters because it is an ionic channel and because the two NBDs are thought to play a major role in the channel gating, i.e. opening and closing [20,27–30]. Until recently, most of the attention has been paid to the ATP-dependent gating of CFTR through patch-clamp and mutagenesis analysis of amino acids at Walker A domains, arguing for functional interdependence between NBD1 and NBD2 [20,23,24,27,28]. This suggested that ATP hydrolysis at NBD1 contributes to channel opening, while hydrolysis at NBD2 leads to closing [28]. However, recent biochemical studies indicated differential interactions of nucleotides at the two NBDs, and that nucleotides bind stably and dissociate slowly from NBD1, while NBD2 rapidly hydrolyses nucleotides [29,30]. A more general mechanism of regulation of CFTR and other ABC transporters by the LSGGQ motif recently emerged from analysis of the crystallographic structures of HisP and other nucleotide-binding proteins. Jones and George in 1999 [3] made the attractive hypothesis that the conserved signature sequence in each NBD may interact with the Walker A site in the opposite NBD. Later, experimental data collected from numerous studies of Rad50 [4], HisP [5], $MalFGK_2$ [6], P-gp [7], MJ0796 [8] and Mdl1p [9] ABC transporters supported this model.

From our results, we propose a plausible mechanism of action of genistein as an intermediate for the cross-talk between the LSGGQ motif and the Walker A domain of the opposite NBDs of CFTR. The first step corresponds to the binding of genistein at G1349 favouring the interaction of LSHGH with the Walker A domain at NBD1 and resulting in MgATP-dependent opening of CFTR chloride channels according to current gating model [20,27,28]. A second molecule of genistein could then binds at G551. The LSGGQ motif triggers the closing of CFTR channels through interaction with the Walker A domain at NBD2. With the G551D mutant, the glycine G1349 being still free to accept a molecule of genistein, the channel can be activated without inhibition at high concentration (because the inhibitory glycine at position 551 has been mutated into aspartate). This may be explained by an interaction of the LSGGQ domain with the Walker A at NBD2 that might controls the inhibition of CFTR channels. On the contrary, with the mutant G1349D the activation of CFTR was abolished. This is an indication of an interaction between LSHGH and the Walker A of NBD1 that controls the

activation of CFTR channels. In support for our hypothesis, an elegant study on P-gp recently suggested that drug-stimulated ATPase activity of P-gp could bring the Walker A and LSGGQ sites closer enough so that ATP hydrolysis occurs at a faster rate [31]. Whether a similar mechanism occurs for CFTR is not known but is certainly attractive although additional experiments will be required.

In conclusion, our study reveals that the symmetrical (but not equivalent) LSGGQ and LSHGH signature motifs control the inhibition and activation of CFTR chloride channels possibly by acting like molecular switches able to turn on and off CFTR via interaction of genistein with its high affinity activatory site located at G1349 in NBD2 and with its low affinity inhibitory site located at G551 in NBD1. Our results also reveal a novel possibility for the development of LSHGH-targeted activators or LSGGQ-targeted inhibitors of CFTR. Although it remains to determine how interaction of genistein with the two glycines interferes with binding and/or hydrolysis at NBD1 and two to promote opening and closing of CFTR channels, our results may fit to the dimer "head-to-tail" hypothesis for ABC transporter [3–9,20].

Acknowledgments

We thank Anne Cantereau for her expert assistance in confocal imaging, Drs. K.H. Karlson and B.A. Stanton for the generous gift of pS65T/EGFP-C1/wt-CFTR construct, Marlène Baudis for the delF508-CFTR construct, N. Bizard and C. Jougla for assistance in cell culture. This work was performed as part of the DEA project of P. Melin at ICBG thesis school at Poitiers University with a scholarship from Région Poitou-Charentes. This work was supported by specific grants from CF-Pronet and Vaincre La Mucoviscidose and institutional grant from the CNRS and Région Poitou-Charentes.

References

[1] Linton KJ, Rosenberg MF, Kerr ID, Higgins CF. Structure of ABC Transporters. In: Holland IB, Cole S, Kuchler K, Higgins CF editors. ABC proteins: from bacteria to man. Academic Press, 2003. p.65–80.
[2] Walker JE, Saraste M, Runswick MJ, Gay NJ. Distantly related sequences in the alpha- and beta-subunits of ATP synthase, myosin, kinases and other ATP-requiring enzymes and a common nucleotide binding fold. EMBO J 1982;1:945–51.
[3] Jones MP, George AM. Subunit interactions in ABC transporters: towards a functional architecture. FEMS Microbiol Lett 1999;179:187–202.
[4] Hopfner KP, Karcher A, Shin DS, Craig L, Arthur LM, Carney JP, et al. Structural biology of Rad50 ATPase: ATP-driven conformational control in DNA double-strand break repair and the ABC-ATPase superfamily. Cell 2000;101:789–800.
[5] Jones MP, George AM. Mechanism of ABC transporters: A molecular dynamics simulation of well characterized nucleotide-binding subunit. Proc Natl Acad Sci USA 2002;99:12639–44.
[6] Fetsch EE, Davidson AL. Vanadate-catalyzed photocleavage of the signature motif of an ATP-binding cassette (ABC) transporter. Proc Natl Acad Sci USA 2002;99:9685–90.
[7] Loo TW, Bartlett MC, Clarke DM. The "LSGGQ" motif in each nucleotide-binding domain of human P-glycoprotein is adjacent to the opposing walker A sequence. J Biol Chem 2002;277:41303–6.
[8] Moody JE, Millen L, Binns D, Hunt JF, Thomas PJ. Cooperative, ATP-dependent association of the nucleotide binding cassettes during the catalytic cycle of ATP-binding cassette transporters. J Biol Chem 2002;277:21111–4.
[9] Janas E, Hofacker M, Chen M, Gompf S, van der Does C, Tampe R. The ATP hydrolysis cycle of the nucleotide-binding domain of the mitochondrial ATP-binding cassette transporter Mdl1p. J Biol Chem 2003;278:26862–9.
[10] Hanrahan JW, Gentzsch M, Riordan JR. The cystic fibrosis transmembrane conductance regulator (ABCC7). In: Holland IB, Cole S, Kuchler K, Higgins CF editors. ABC proteins: from bacteria to man. Academic Press, 2003. p. 589–618.
[11] Riordan JR, Rommens JM, Kerem B, Alon N, Rozmahel R, Grzelczak Z, et al. Identification of the cystic fibrosis gene: cloning and characterization of complementary DNA. Science 1989;245:1066–73.
[12] Quinton PM. Physiological basis of cystic fibrosis: a historical perspective. Physiol Rev 1999;79:S3–S22.
[13] Welsh MJ, Smith AE. Molecular mechanisms of CFTR chloride channel dysfunction in cystic fibrosis. Cell 1993;73:1251–4.
[14] Cutting GR, Kasch LM, Rosenstein BJ, Zielensky J, Tsui L-C, Antonarakis SE, et al. A cluster of Cystic Fibrosis mutations in the first nucleotide binding fold domain of the Cystic Fibrosis conductance regulator protein. Nature 1990;346:366–9.
[15] Chang XB, Tabcharani JA, Hou YX, Jensen TJ, Kartner N, Alon N, et al. Protein kinase A (PKA) still activates CFTR chloride channel after mutagenesis of all 10 PKA consensus phosphorylation sites. J Biol Chem 1993;268:11304–11.
[16] Logan J, Hiestand D, Daram P, Huang Z, Muccio DD, Hartman J, et al. Cystic fibrosis transmembrane conductance regulator mutations that disrupt nucleotide binding. J Clin Invest 1994;94:228–36.
[17] Li C, Ramjeesingh M, Wang W, Garami E, Hewryk M, Lee D, et al. ATPase activity of the cystic fibrosis transmembrane conductance regulator. J Biol Chem 1996;271:28463–8.
[18] Howell LD, Borchardt R, Cohn JA. ATP hydrolysis by a CFTR domain: pharmacology and effects of G551D mutation. Biochem Biophys Res Commun 2000;271:518–25.
[19] Dérand R, Bulteau-Pignoux L, Becq F. The cystic fibrosis mutation G551D alters the non-Michaelis–Menten behaviour of the cystic fibrosis transmembrane conductance regulator (CFTR) channel and abolishes the inhibitory Genistein binding site. J Biol Chem 2002;277:35999–6004.
[20] Vergani P, Nairn AC, Gadsby DC. On the mechanism of MgATP-dependent gating of CFTR Cl^- channels. J Gen Physiol 2003;121:17–36.
[21] Moyer BD, Loffing J, Schwiebert EM, Loffing-Cueni D, Halpin PA, Karlson KH, et al. Membrane trafficking of the cystic fibrosis gene product, cystic fibrosis transmembrane conductance regulator, tagged with green fluorescent protein in madin-darby canine kidney cells. J Biol Chem 1998;273:21759–68.
[22] Dérand R, Bulteau-Pignoux L, Mettey Y, Zegarra-Moran O, Howell LD, Randak C, et al. Activation of G551D CFTR channel with MPB-91: regulation by ATPase activity and phosphorylation. Am J Physiol Cell Physiol 2001;281:C1657–66.
[23] Smit LS, Wilkinson DJ, Mansoura MK, Collins FS, Dawson DC. Functional roles of the nucleotide-binding folds in the activation of the cystic fibrosis transmembrane conductance regulator. Proc Natl Acad Sci USA 1993;90:9963–7.
[24] Wilkinson DJ, Mansoura MK, Watson PY, Smit LS, Collins FS, Dawson DC. CFTR: the nucleotide binding folds regulate the acces-

sibility and stability of the activated state. J Gen Physiol 1996;107: 103–19.
[25] Denning GM, Anderson MP, Amara JF, Marshall J, Smith AE, Welsh MJ. Processing of mutant cystic fibrosis transmembrane conductance regulator is temperature-sensitive. Nature 1992;358:761–4.
[26] Dalemans W, Barbry P, Champigny G, Jallat S, Dott K, Dreyer D, et al. Altered chloride ion channel kinetics associated with the delta F508 cystic fibrosis mutation. Nature 1991;354:526–8.
[27] Cotten JF, Welsh MJ. Covalent modification of the nucleotide binding domains of cystic fibrosis transmembrane conductance regulator. J Biol Chem 1998;273:31873–9.
[28] Gadsby DC, Nairn AC. Control of CFTR channel gating by phosphorylation and nucleotide hydrolysis. Physiol Rev 1999;79:S77–S107.
[29] Aleksandrov L, Mengos A, Chang X, Aleksandrov A, Riordan JR. Differential interactions of nucleotides at the two nucleotide binding domains of the cystic fibrosis transmembrane conductance regulator. J Biol Chem 2001;276:12918–23.
[30] Aleksandrov L, Aleksandrov AA, Chang XB, Riordan JR. The first nucleotide binding domain of cystic fibrosis transmembrane conductance regulator is a site of stable nucleotide interaction, whereas the second is a site of rapid turnover. J Biol Chem 2002;277: 15419–25.
[31] Loo TW, Bartlett MC, Clarke DM. Drug binding in human P-glycoprotein causes conformational changes in both nucleotide-binding domains. J Biol Chem 2003;278:1575–8.